(9) Tashiro, K.; Takano, K.; Kobayashi, M.; Chatani, Y.; Tadokoro, H. *Polymer* **1981**, *22*, 1312; **1984**, *25*, 195; *Ferroelectrics* **1984**, *57*, 297.
(10) Davis, G. T.; Furukawa, T.; Lovinger, A.; Broadhurst, M. G. *Macromolecules* **1982**, *15*, 323, 329.
(11) Lovinger, A.; Furukawa, T.; Davis, G. T.; Broadhurst, M. G. *Polymer* **1983**, *24*, 1225, 1233; *Ferroelectrics* **1983**, *50*, 227.
(12) Tashiro, K.; Kobayashi, M. *Polymer* **1986**, *27*, 667.
(13) Ohigashi, H.; Koga, K. *Jpn. J. Appl. Phys.* **1982**, *21*, L455.
(14) Tajitsu, Y.; Date, M.; Furukawa, T.; Hantani, H.; Ogura, H.; Chiba, A. *Polym. Prepr. Jpn.* **1984**, *33*, 2587.
(15) Tajitsu, Y.; Ogura, H.; Chiba, A.; Furukawa, T. *Jpn. J. Appl. Phys.* **1987**, *26*, 554.
(16) Vonk, C. G. In *Small Angle X-ray Scattering*; Glatter, O., Kratky, A., Eds.; Applied Science: Essex, England, 1982.
(17) Porod, G. *Kolloid, Z. Z. Polym.* **1957**, *125*, 51, 108.
(18) Vonk, C. G. *J. Appl. Crystallogr.* **1973**, *6*, 81.
(19) Bunn, C. W.; Cobbold, A. J.; Palmer, R. P. *J. Polym. Sci.* **1958**, *28*, 365.
(20) Matsushige, K.; Enoshita, R.; Ide, T.; Yamauchi, N.; Taki, S.; Takemura, T. *Jpn. J. Appl. Phys.* **1977**, *16*, 681.
(21) Wunderlich, B.; Arakawa, T. *J. Polym. Sci., Part A* **1964**, *1*, 1245.
(22) Geil, P. H. *J. Polym. Sci. Part A* **1964**, *2*, 3813.
(23) Miyamoto, Y.; Nakafuku, C.; Takemura, T. *Polym. J.* **1972**, *3*, 120.
(24) Bassett, D. C. In *Developments in Crystalline Polymers-1*; Bassett, D. C., Ed.; Applied Science: Essex, England, 1982.
(25) Ohigashi, H.; Koga, K.; Suzuki, M.; Nakanishi, T.; Kimura, K.; Hashimoto, N. *Ferroelectrics*. **1984**, *60*, 263.

Polymer Scission with Irreversible Reattachment: A Kinetic Model of Pyrolysis with Char Formation

Alan R. Kerstein*

Sandia National Laboratories, Livermore, California 94550

Stephen Niksa

High Temperature Gasdynamics Laboratory, Mechanical Engineering Department, Stanford University, Stanford, California 94305. *Received November 17, 1986*

ABSTRACT: The pyrolitic degradation of polymers is modeled by the simultaneous processes of bond scission and irreversible monomer reattachment applied to linear chains or branching (loopless) networks. The monomer, or elemental unit, of the network is assumed to be the common precursor of volatiles (tar), formed by a first-order rate process, and refractory solids (char), formed by monomer reattachment to any broken bond. A closed set of rate equations governing this model is derived. Exemplary cases are solved, and a previous application of this model to coal devolatilization is discussed. The predicted dependence of tar and char yields on heating rate, a consequence of network statistics in conjunction with temperature-dependent reaction rates, is consistent with devolatilization measurements and may be relevant to other pyrolysis processes. The network version of the model exhibits a percolation transition which may represent the softening transition observed during the pyrolysis of some coals.

1. Introduction

Recent analyses of polymer degradation kinetics have focused primarily on two issues. First, the steady-state size distribution has been analyzed for polymers subject to simultaneous scission and reattachment processes, with both processes reversible.[1,2] Second, the complete transient evolution has been analyzed for a class of linear-chain models of polymers subject to irreversible scission with no reattachment.[3] Here we consider the complete transient evolution of a class of linear-chain and branching (loopless) network models subject to scission with irreversible reattachment.

The analysis is motivated by certain features of pyrolysis processes in which volatiles (tar) and refractory solids (char) are produced. As a concrete example, we consider the application to coal devolatilization that originally motivated the analysis.[4] Transient and ultimate tar and char yields during the thermal decomposition of coal have traditionally been modeled by postulating a small number of species classes, or lumps, in the unreacted coal which react according to a simple chemical-kinetic scheme. These lumps are converted to product either directly or through a reactive intermediate (metaplast) according to a scheme with phenomenologically assigned stoichiometric coefficients and temperature-dependent (typically Arrhenius) rate coefficients.

Motivated by recent progress in the development of a macromolecular picture of coal structure,[5] we have formulated[4] a pyrolysis model in which the reactive intermediate is the elemental unit (monomer) in a network representing the unreacted coal. Pyrolytic decomposition is represented by scission of network bonds. After an individual monomer is freed, i.e., fully detached from its neighbors, it is subject to two competing processes. One process is conversion to tar (which escapes from the system) according to a first-order rate process. The other process is irreversible reattachment to any broken bond. The irreversible nature of this reattachment reflects the refractory nature of the char which is formed during pyrolysis. The stability of the reattached bonds results in inhibition of the rate of free monomer release for a given bond-scission rate. This inhibition introduces a dynamic feedback effect of char formation on the production of free monomers. The quantitative impact of this feedback, which is governed by the statistics of network fragmentation, is the key feature of the model which has led to an enhanced capability to predict heating-rate dependences of transient and ultimate yields measured over a wide range of experimental conditions.[6-8]

The previously presented formulation[4] of our network model of pyrolysis incorporated additional features, such as dangling side branches, intended to represent aspects

0024-9297/87/2220-1811$01.50/0

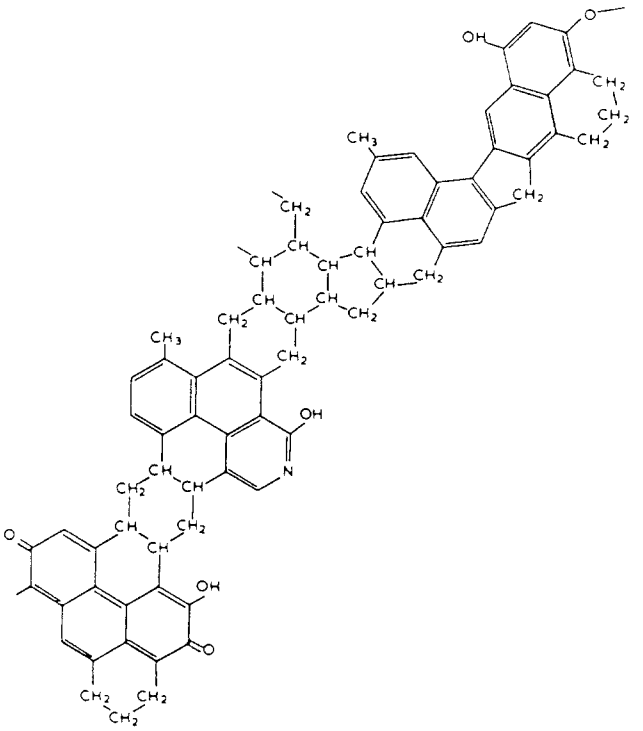

Figure 1. Structure of a typical segment of the coal macromolecule (adapted from ref 9).

of macromolecular structure specific to the coal application. Since our objective here is to identify the underlying dynamics of the coupling between the processes of monomer release and reattachment in a more general context, these application-specific features are omitted. Also omitted are detailed mechanistic justifications of model assumptions, which are presented elsewhere.[4,6] The focus here is on mathematical derivation of a closed set of rate equations governing the network pyrolysis model and interpretation of the trends and parameter dependences that are obtained.

For concreteness, the molecular structure of a typical segment of the coal macromolecule, as presently understood,[9] is illustrated in Figure 1. An aromatic unit consisting of two such segments corresponds to a monomer in the present context. Neighboring monomers may be linked either by ether bridges (such as the oxygen atom in the upper right-hand corner of the figure) or by aliphatic structures (such as the alicyclic ring in the center of the figure). These linking structures are subject to pyrolitic decomposition during devolatilization. Since these linking structures appear also in the interiors of aromatic units, it is evident that there is some arbitrariness in the specification of individual monomers. The operational definition is based on the maximum molecular weight for which the unit may be regarded as sufficiently mobile so that its interactions can be modeled as chemical rate processes. Similarly, tar is operationally defined as any aromatic structure (including aliphatic linkages) small enough so that its vaporization rate exceeds chemical rates for its reattachment or further decomposition. The segment illustrated in Figure 1 is comprised of two typical tar structures, linked by the aliphatic ring in the center of the figure. These operational definitions are applicable over limited ranges of temperature and pressure, which influence the vaporization and chemical rates.[7]

The reattachment process typically consists of the reintegration of the remnants of two pyrolyzed aliphatic linkages into a more stable structure such as an aromatic ring. The incipient char structure is further stabilized, e.g., by means of thermally induced graphitization of the aromatic backbone, which generates hydrogen gas. The latter aspect is omitted from the model since it does not appreciably affect the competition determining the final product distribution.

2. Model Formulation

We model the unreacted polymer as a z-coordinated Bethe lattice[10,11] (a branched, loopless network), with each site representing a monomeric unit. Each site is assigned unit mass. To avoid complications associated with branching, we initially specialize to $z = 2$, i.e., a linear chain. The linear chain captures the features of principal interest, as noted later.

The bonds initially connecting pairs of sites are denoted as bridges to distinguish them from char bonds formed later by the reattachment process. No mass is assigned to bridges or char bonds.

Polymer degradation is represented by the process of bridge scission, with a scission rate k_S per bridge. Unless noted otherwise, this and all other rate parameters, as well as all state variables, are time dependent. This dependence may be either explicit or implicit, e.g., through the dependence of rate parameters on the time-varying temperature of the system. The scission process decomposes the linear chain into polymer fragments, or finite sequences of sites connected in succession by unbroken bridges, with a broken bridge at each end of a fragment.

When both bridges emanating from a given site have been broken, the site is designated as a free monomer and either of its broken bridges can then reattach to any other broken bridge. Reattachment is modeled as a second-order rate process, with a rate linear in both the free monomer and broken-bridge concentrations and with rate coefficient k_C. Every reattachment involves (at least) one free monomer, based on the assumption that free monomer is the only mobile species. (In effect, free monomer is a lumped representation of all mobile species comprising the reactive intermediate.) Sites joined by the char bonds formed upon reattachment are deemed to have been converted from unreacted polymer to char. Sites are thus partitioned into three species: free monomers (with two broken bridges), char (with at least one char bond), and unreacted polymer (with at least one unbroken bridge and no char bonds). The tar formation process, incorporated into the model in section 3, introduces an additional species. For now, tar formation is omitted and mass partitioning is based on these three species.

Monomers are taken to be two-coordinated with respect to char bonds as well as bridges, so the reattachment process results in the growth of linear chain segments, each comprised of sites connected in succession by char bonds, terminated by a broken bridge. Such a segment may be initiated by free monomer reattachment at either end of a polymer fragment or may be initiated by monomer–monomer reattachment. The monomer-fragment reattachment process results in the formation of fragments containing a sequence of bridges, with a char segment (i.e., a sequence of char bonds, terminated by a broken bridge) at either or both ends. The monomer–monomer reattachment process initiates a pure char fragment, containing no unbroken bridges. A pure char fragment can also be formed by the scission of a bridge adjacent to a char segment.

A complete characterization of the structure of a fragment requires three parameters c_1, c_2, and x, where x is the number of unbroken bridges in the fragment and c_1 and c_2 are the number of char bonds at either end. Fragment structure may be denoted as $[c_1 \cdot \underline{x} \cdot c_2]$, as in

Scheme I
Fragment Structure, Typical Processes, and Rate Coefficients for the Linear Chain[a]

fragment or species type	notation	number density
fragment with $\underline{x}$ bridges and no char segments	$[\underline{x}]$	$n(\underline{x},0)$ $(\underline{x} > 0)$
fragment with $\underline{x}$ bridges and one char segment with c_1 char bonds	$[c_1\cdot\underline{x}]$	$n(\underline{x},1)$ $(\underline{x} > 0)$
fragment with $\underline{x}$ bridges and two char segments	$[c_1\cdot\underline{x}\cdot c_2]$	$n(\underline{x},2)$ $(\underline{x} > 0)$
pure char fragment	$[c_1]$	$n(0,1)$
free monomer	F	$n(0,0) = N_F$
tar	T	N_T

Typical Processes and Rate Coefficients

dissociation of fragment with one char segment

$$[\underline{c_1}\cdot\underline{x}]\begin{cases}\xrightarrow{k_S} [\underline{c_1}] + [\underline{x-1}]\\ \xrightarrow{k_S} [\underline{c_1}\cdot\underline{x-y}] + [\underline{y-1}] \quad (1 < \underline{y} < \underline{x})\\ \xrightarrow{k_S} [\underline{c_1}\cdot\underline{x-1}] + \mathrm{F}\end{cases}$$

reattachment

$$\mathrm{F} + \mathrm{F} \xrightarrow{k_C} [1]$$

$$[\underline{c_1}] + \mathrm{F} \xrightarrow{k_C} [\underline{c_1} + 1]$$

$$[\underline{x}] + \mathrm{F} \xrightarrow{k_C} [1\cdot\underline{x}]$$

$$[\underline{c_1}\cdot\underline{x}] + \mathrm{F}\begin{cases}\xrightarrow{k_C} [\underline{c_1} + 1\cdot\underline{x}]\\ \xrightarrow{k_C} [\underline{c_1}\cdot\underline{x}\cdot 1]\end{cases}$$

$$[\underline{c_1}\cdot\underline{x}\cdot\underline{c_2}] + \mathrm{F}\begin{cases}\xrightarrow{k_C} [\underline{c_1} + 1\cdot\underline{x}\cdot\underline{c_2}]\\ \xrightarrow{k_C} [\underline{c_1}\cdot\underline{x}\cdot\underline{c_2} + 1]\end{cases}$$

tar formation

$$\mathrm{F} \xrightarrow{k_T} \mathrm{T}$$

[a] Brackets delimit fragments; the number of bridges in a fragment is underscored; raised dots delimit char segments within fragments.

Scheme I. c_1 and c_2 are interchangeable, so we specify $0 \le c_1 \le c_2$. For a pure char fragment, $x = 0$ and only the total number c of char bonds need be specified.

For a complete statistical characterization of the instantaneous state of the system, the number density of each distinct fragment structure, parametrized by c_1, c_2, and x, must be specified. However, if only a mass partitioning is required, based on the relative numbers of unreacted-polymer sites, free monomers, and char sites, then it suffices to characterize fragments in terms of x and the number $i = 0$, 1, or 2 of attached char segments. The instantaneous number density of fragments with given x and i is denoted $n(x, i)$. (To simplify notation, time dependence is suppressed in this and other definitions.) All number densities are expressed on a per-site basis, so $n(x, i)$ may be interpreted as the ratio of the number of type (x, i) fragments to the total number of sites in the system. (The total number of sites is nominally infinite, but no difficulties arise because only ratios are considered.)

For $x = 0$, the notation is ambiguous. We resolve the ambiguity by denoting the free monomer number density as $n(0,0)$ and the number density of pure char fragments as $n(0,1)$.

On the basis of these definitions and notations, processes governing the evolution of fragment structure are illustrated in Scheme I. (These processes are analyzed in detail in section 3.) Dissociation pathways are shown only for type $(x,1)$ fragments since the pathways for other fragment types are quite similar.

Returning to the partition into species, we introduce the number densities N_U, N_F, and N_C of unreacted polymer, free monomer, and char sites, respectively. On the basis of our assignment of unit mass to each site, these number densities are interpreted as mass fractions of the respective species. (In these and other definitions, number densities representing mass fractions are designated by uppercase N.)

Equations governing the evolution of the system are most conveniently derived in terms of the fragment number densities $n(x,i)$, which must then be related to the species mass fractions. It follows from the foregoing definitions that $N_F = n(0,0)$. To obtain N_U, we note that a fragment with $x > 0$ unbroken bridges has at least $x - 1$ unreacted-polymer sites. It has an additional unreacted-polymer site at each end which has not undergone monomer-fragment reattachment. Therefore a type (x,i) fragment has $x + 1 - i$ unreacted-polymer sites. Summation over fragment types give

$$N_U = \sum_{x=1}^{\infty}\sum_{i=0}^{2}(x + 1 - i)n(x,i) \tag{1}$$

Finally, N_C can be obtained from the mass-fraction normalization $N_U + N_F + N_C = 1$. This normalization is generalized in section 3 to include a tar species.

3. Rate Equations

A rate equation governing each of the number densities $n(x,i)$ is obtained by considering the mechanisms for creation and depletion of each type of fragment. For instance, a fragment with $x > 0$ and $i = 0$ can be created by scission of a bridge in a fragment with y bridges, where $y > x$, and with $i = 0$ or 1 attached char segments. If the parent fragment has $i = 1$ (i.e., one char segment), then there is only one bridge whose scission will produce a type $(x,0)$ fragment [and in addition, will produce a type $(y-x-1,1)$ fragment]. If the parent fragment has $i = 0$, with $y \neq 2x + 1$, then scission of either of two bridges will yield one fragment each of types $(x,0)$ and $(y-x-1,0)$, where $y - x - 1 \neq x$. If the parent is type $(2x+1,0)$, then scission of the central bridge will yield two $(x,0)$ fragments. This completes the enumeration of sources of $(x,0)$ fragments for $x > 0$.

The two mechanisms for depletion of $(x,0)$ fragments are (1) scission of any one of the x bridges, yielding a fragment pair $(y,0)$ and $(x-y-1,0)$, where $0 \le y < x$, and (2) free monomer reattachment to the broken bond at either end, yielding a type $(x,1)$ fragment. On the basis of the rate processes assumed to govern the scission and reattachment mechanisms, the aforementioned contributions to creation and depletion of type $(x,0)$ fragments may be combined to obtain

$$\frac{dn(x,0)}{dt} = 2k_S\sum_{y=x+1}^{\infty}n(y,0) + k_S\sum_{y=x+1}^{\infty}n(y,1) - k_S x n(x,0) - 2k_C n(0,0)n(x,0); \qquad x > 0 \tag{2}$$

Analogous considerations lead to formulation of the rate equations

$$\frac{dn(x,1)}{dt} = k_S\sum_{y=x+1}^{\infty}n(y,1) + 2k_S\sum_{y=x+1}^{\infty}n(y,2) + 2k_C n(0,0)n(x,0) - k_S x n(x,1) - k_C n(0,0)n(x,1); \qquad x > 0 \tag{3}$$

and

$$\frac{dn(x,2)}{dt} = k_C n(0,0) n(x,1) - k_S x n(x,2); \qquad x > 0 \quad (4)$$

Two features of eq 3 and 4 are noteworthy. First, the reattachment mechanism contributes both source and sink terms in eq 3, while it contributes only a source term in eq 4. Second, bridge scission contributes only a sink term in eq 4 because fragments created by scission cannot have $i = 2$ (though subsequent reattachment events may increment their i values).

Next, the rate equation for free monomers is considered. The free monomer sources are analogous to those of eq 2. The depletion mechanisms are reattachment and tar formation. Since reattachment is a second-order rate process, it contributes a depletion term proportional to the free monomer number density $n(0,0)$ times the number density of broken bridges. Each fragment, including free monomer, has a broken bridge at each end, so the broken-bridge number density is twice the total number density of all fragment types. Combining terms, we obtain

$$\frac{dn(0,0)}{dt} = 2k_S \sum_{y=1}^{\infty} n(y,0) + k_S \sum_{y=1}^{\infty} n(y,1) - 2k_C n(0,0) \sum_{y=1}^{\infty} \sum_{i=0}^{2} n(y,i) - 2k_C n(0,0) n(0,1) - 2k_C n^2(0,0) - k_T n(0,0) \quad (5)$$

Here, tar formation is incorporated into the model as a first-order rate process depleting the free monomer number density, with rate coefficient k_T. This formulation is motivated by mechanisms presumed to govern the coal devolatilization process.[4,6]

Finally, the rate equation for pure char fragments is

$$\frac{dn(0,1)}{dt} = k_S \sum_{y=1}^{\infty} n(y,1) + 2k_S \sum_{y=1}^{\infty} n(y,2) + k_C n^2(0,0) \quad (6)$$

The first two terms are analogous to source terms in eq 3. The last term represents the initiation of one pure char segment per monomer–monomer reattachment. There are no depletion terms for pure char, reflecting the irreversibility of the reattachment process.

It is convenient to define an additional set of state variables $n(x) = \sum_{i=0}^{2} n(x,i)$ representing the number density of fragments containing x bridges, irrespective of the number of attached char segments. Equations 2–4 can then be summed to give the following set of rate equations involving only the state variables $n(x)$:

$$\frac{dn(x)}{dt} = 2k_S \sum_{y=x+1}^{\infty} n(y) - k_S x n(x); \qquad x > 0 \quad (7)$$

There are no reattachment terms in this equation due to cancellation. This result reflects the fact that reattachment does not change the number of bridges in a fragment. The time evolution of the state variables $n(x)$ is governed solely by the bridge-scission process.

Since scissions are random, independent events in our modeling framework, the latter observation motivates a simple approach to solving the initial-value problem for the quantities $n(x)$. At any time t, the number of density $n(x)$ of x-bridge fragments depends only on the fraction K of bridges broken as of time t. For given K, elementary application of the statistical theory of runs[12] gives

$$n(x) = K^2(1 - K)^x \quad (8)$$

This result may be derived by interpreting $n(x)$ as the probability that a given bridge is the left-most bridge of an x-bridge fragment. That probability is equal to the probability $(1 - K)^x$ that the given bridge and its $x - 1$ neighbors to the right are unbroken, times the probability K^2 that the adjacent bridges on either side of the fragment are broken.

To complete the solution for $n(x)$, K must be expressed in terms of the bridge-scission rate k_S. The rate $\dot{K}$ of accumulation of broken bridges is the scission rate k_S per unbroken bridge times the fraction $1 - K$ of remaining unbroken bridges. K thus evolves according to the differential equation $\dot{K} = k_S(1 - K)$. For the initial condition $K = 0$, the solution of this equation is

$$K = 1 - \exp\left[-\int_0^t k_S(t')\, dt'\right] \quad (9)$$

It can be verified by direct substitution that eq 8 and 9 satisfy eq 7. This solution for $n(x)$ is now exploited to reduce eq 1–6 to a closed set of rate equations.

Using eq 8, we can evaluate two of the sums on the right-hand side of eq 1, namely

$$n_B \equiv \sum_{x=1}^{\infty} n(x) = K(1 - K) \quad (10)$$

and

$$\sum_{x=1}^{\infty} x n(x) = 1 - K \quad (11)$$

(n_B is the number density of bridge-containing fragments, i.e., fragments other than free monomer or pure char.) The third sum on the right-hand side of eq 1 is the total number density of char segments attached to fragments with $x > 0$. This quantity is denoted as an additional state variable, $n_R = \sum_{x=1}^{\infty} \sum_{i=0}^{2} i n(x,i)$. In terms of these results and definitions, eq 1 can be reexpressed as

$$N_U = 1 - K^2 - n_R \quad (12)$$

A rate equation for n_R is obtained by multiplying both sides of eq 4 by 2, adding the result to eq 3, and summing over $x > 0$. Evaluating sums using the identity $\sum_{x=1}^{\infty} \sum_{y=x+1}^{\infty} f(y) = \sum_{x=1}^{\infty} (x - 1) f(x)$ and recalling the notation $N_F = n(0,0)$ for the free monomer number density, we obtain

$$\frac{dn_R}{dt} = k_C[2n_B - n_R]N_F - k_S n_R = k_C[2K(1 - K) - n_R]N_F - k_S n_R \quad (13)$$

(This equation can be derived directly by enumerating the creation and depletion mechanisms for char segments attached to fragments.) Similarly, eq 5 can be reexpressed as

$$\frac{dN_F}{dt} = k_S[2K(1 - K) - n_R] - 2k_C[K(1 - K) + n_P]N_F - 2k_C N_F^2 - k_T N_F \quad (14)$$

Here, the notation $n_P = n(0,1)$ for the number density of pure char fragments has been introduced. The free monomers lost to tar formation are assigned to a tar species N_T governed by the rate equation

$$\frac{dN_T}{dt} = k_T N_F \quad (15)$$

Finally, eq 6 can be reexpressed as

$$\frac{dn_P}{dt} = k_S n_R + k_C N_F^2 \quad (16)$$

The rate equations 13–16, in conjunction with the algebraic relation 12, eq 9 for K, and the initial conditions $N_U = 1$ and $n_R = n_P = N_F = N_T = 0$ constitute a well-posed

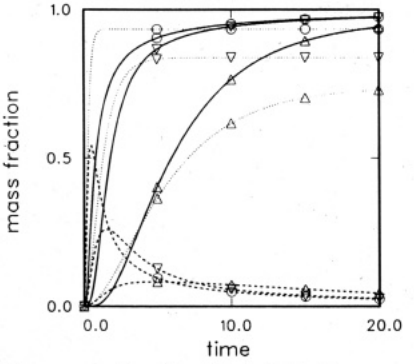

Figure 2. Char mass fraction N_C (solid), free monomer mass fraction N_F (dashed), and gross free monomer production N_G (dotted) vs. time, computed with the linear-chain model with rate coefficients $k_C = 1$, $k_T = 0$, and $k_S = 0.2$ (△), 1 (▽), and 5 (○).

initial-value problem determining the time-dependent mass fractions N_U, N_F, and N_T of unreacted polymer, free monomer, and tar, respectively, and the additional quantities n_R and n_P. Since all sites not assigned to one of the above three mass fractions must be char sites, the char mass fraction N_C is determined by the mass closure

$$N_U + N_F + N_C + N_T = 1 \tag{17}$$

Solution of this initial-value problem determines the time evolution of the mass partition into the four constituents appearing in eq 17. Additional detail concerning the number densities of fragment species can be obtained by solving eq 2–6 for all the quantities $n(x,i)$. As noted earlier, even this set of state variables does not provide a complete statistical characterization of all fragment species.

In light of these results, we comment further on the distinction between purely chemical-kinetic schemes and our model, which incorporates chain statistics (generalized to network statistics in section 5). The infinite hierarchy of rate equations given by eq 2–6 is formally indistinguishable from a chemical-kinetic scheme. The solution, eq 8 and 9, of the hierarchy of evolution equations for the state variables $n(x)$ could have been introduced without reference to chain statistics, leading to the closed set of equations finally obtained. The key point is that the hierarchy of equations for $n(x)$ constitutes an alternative representation of chain fragmentation due to random bridge breaking, as governed by the statistical theory of runs. Chain statistics provide the most direct route to the solution for $n(x)$. The appearance of terms involving the quantity K is the explicit manifestation of chain statistics in the final equations.

4. Exemplary Solutions

The principal dynamical feature of our pyrolysis model is the inhibiting effect of reattachment on the production of free monomers. The principal consequence of this feature is its influence on the competition between char and tar production.

To illustrate the dynamics of monomer production and reattachment, Figure 2 shows computed transient solutions of eq 9 and 12–16 for several values of k_S, with k_C normalized to unity and with tar formation omitted; i.e., $k_T = 0$. The time profiles of N_C, N_F, and gross free monomer production

$$N_G = \int_0^t k_S[2K(1 - K) - n_R]\, dt' \tag{18}$$

are plotted. The latter quantity, a time integral of the source term of eq 14, is the total number density of sites which evolve to free monomer some time during the interval $[0,t]$, including those which reattach prior to t. In the limit of small k_S, the instantaneous free monomer concentration vanishes but N_G converges at large t to the value $^2/_3$. Thus, reduction of k_S lengthens the time interval of transient evolution, severely reducing the peak free monomer concentration but with a less severe reduction of gross free monomer production.

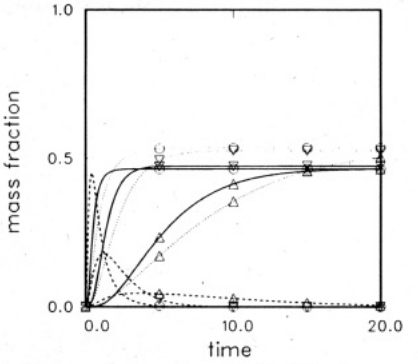

Figure 3. Char mass fraction N_C (solid), free monomer mass fraction N_F (dashed), and tar mass fraction N_T (dotted) vs. time, computed with the linear-chain model with $k_C = k_T = 1$ and $k_S = 0.2$ (△), 1 (▽), and 5 (○).

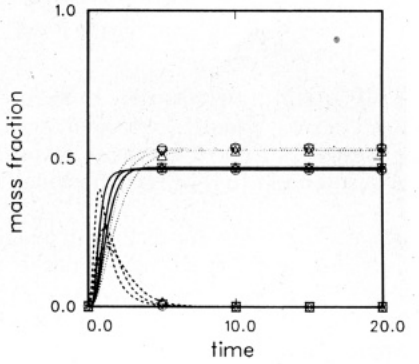

Figure 4. Char mass fraction N_C (solid), free monomer mass fraction N_F (dashed), and tar mass fraction N_T (dotted) vs. time, computed with the linear-chain model with $k_C = k_T = 1$ and $k_S = 1 + At$, where $A = 0.2$ (△), 1 (▽), and 5 (○).

Gross free monomer production is reduced at small k_S because monomer–fragment reattachments inhibit further monomer production. An unreacted-polymer site at the end of a fragment can be released as free monomer upon scission of its remaining unbroken bridge, but reattachment at that site prior to scission of the bridge irreversibly converts the site to char. Therefore if k_S is infinite, i.e., all bridges break before any reattachments, then gross free monomer production is unity, but for finite k_S, gross free monomer production is lower.

The influence of scission-reattachment dynamics on the competition between char and tar formation is illustrated in Figures 3–5. k_T and k_C are both fixed at unity, so variations in the relative yields of these products reflect scission-reattachment dynamics. In Figure 3, k_S is held constant in time for a given computation, but this constant value is changed from run to run. In Figure 4, k_S is assigned a linear time dependence $k_S = 1 + At$, with the parameter A varied from run to run. Thus, Figures 3 and 4 illustrate first the effect of the relative rates of scission and product formation and second the effect of a time-dependent scission rate, as would result from a thermal transient.

Figure 3 and 4 indicate that the principal effect of varying k_S is to vary the time scale for transient evolution, with little impact on ultimate yields. In this regard, the competition between char formation and tar formation

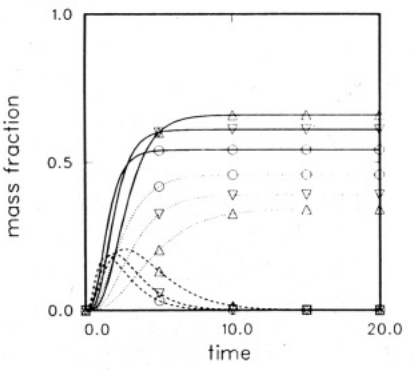

Figure 5. Char mass fraction N_C (solid), free monomer mass fraction N_F (dashed), and tar mass fraction N_T (dotted) vs. time, computed with the linear-chain model with $k_C = \exp(-E_C/\Theta)$, $k_T = \exp(-E_T/\Theta)$, and $k_S = \exp(-E_S/\Theta)$, where the activation-energy parameter values are $E_C = E_S = 1$ and $E_T = 2$. The temperature parameter Θ varies linearly in time according to $\Theta = 1 + Bt$, where $B = 0.2$ (△), 1 (▽), and 5 (○).

produces results qualitatively similar to Figure 2, where competition is absent. Even the transient time scale exhibits little change in Figure 4, where variation of the parameter A is intended to represent heating-rate variation.

The results are dramatically different when the rate coefficients are assigned Arrhenius temperature dependences, $k_y = \exp(-E_y/\Theta)$, where E is a parameter representing activation energy, Θ is a temperature parameter, and y is a generic designator for the subscripts S, C, and T, respectively. For our exemplary computation, we take $E_S = E_C = 1$ and $E_T = 2$. To represent the linear thermal transients employed in many experiments[4,6] we assume $\Theta = 1 + Bt$, where heating rate is represented by the parameter B.

Computed results for several B values are shown in Figure 5. The ultimate yields now exhibit significant dependence on heating rate, with trends in accordance with experimental observations.[4,6] This dependence arises by the following mechanism. At low heating rate, the char formation rate is significantly greater than the tar formation rate during the early portion of the transient, favoring monomer–fragment reattachment. This reattachment process inhibits further monomer release, analogous to the reduction in gross monomer production exhibited in Figure 2. Therefore, relatively few free monomers are available during the latter portion of the transient, when char formation and tar formation rates are roughly equal. At high heating rate, both formation rates reach values near unity before many free monomers are produced, so the overall bias toward char formation is reduced. (In the limit of infinite heating rate, all rate coefficients are equal to unity at all times.)

These results indicate that the dynamic feedback effect of char formation on the production of free monomers, in conjunction with temperature-dependent reaction rates, can account for the observed dependence of product yields on heating rate. The exemplary results presented here are based on modeling assumptions and parameter values chosen to highlight the underlying mechanisms. For quantitative comparisons to experimental data, the model must be augmented to incorporate other relevant aspects of coal devolatilization phenomenology, model parameters must be expressed in physical units, and parameter values must be adjusted to fit the data. These aspects are discussed in detail elsewhere.[4,6-8]

5. Generalization to Branched Networks

To demonstrate that the restriction to linear chains is not essential to either the derivation of rate equations or the dynamics governing the computed trends, we generalize to a representation of the unreacted polymer as a z-coordinated Bethe lattice. The reattachment process can be generalized in several ways. For instance, we can take free monomers to be z-coordinated and thereby allow reattachment to generate a z-coordinated char lattice. However, the statistics of lattice generation in this manner are tractable only by computer simulation, so we adopt an alternative assumption. Namely, free monomers are taken to be two-coordinated and reattachment is not allowed to raise the coordination number of participating sites above 2. Thus, reattachment results in the growth of linear chains, as before.

For the Bethe lattice, it is unwieldy to generate a hierarchy of rate equations with respect to the number x of bridges in a fragment. Therefore we proceed by deriving rate equations individually until a closed set is obtained, guided in our choice of state variables by the results of section 3. We thus obtain equations which determine the mass partitioning but provide no further information concerning the distribution of fragment species.

As before, pure char fragments are initiated by monomer–monomer reattachment or are formed by the scission of a bridge adjacent to a char segment. A char segment is initiated by free monomer reattachment to a "bridge end," i.e., a site with exactly one unbroken bridge and no char bonds. (Without the latter restrictions, reattachment might cause the site to have coordination number greater than 2, in violation of our assumptions.) For $z = 2$, it was convenient to omit explicit consideration of the number density n_E of bridge ends. n_E obeys the relation $n_E + n_R = 2n_B$, with n_B given by eq 10, for $z = 2$. This indicates simply that each bridge-containing fragment has two ends, each of which either is a bridge end or has a char segment attached.

To generalize the relation between n_E and other quantities, we note that for all $z \geq 2$, the sum of n_E and n_R is equal to the number density of sites with exactly one unbroken bridge. For a given site, the probability of this condition is $zK^{z-1}(1 - K)$. (The fraction K of broken bonds is still given by eq 9.) Therefore

$$n_E + n_R = zK^{z-1}(1 - K) \tag{19}$$

Unreacted-polymer sites are depleted only if they are bridge ends. A site which is a bridge end may cease to be a bridge end due to either monomer reattachment at a rate $k_C N_F$ per bridge end or breakage of the remaining bridge at a rate k_S per bridge end. Combining terms and multiplying per-bridge-end quantities by n_E, we obtain

$$\frac{dN_U}{dt} = -k_C n_E N_F - k_S n_E \tag{20}$$

The first depletion term of eq 20 is the source term for char segments, whose number density n_R is now governed by

$$\frac{dn_R}{dt} = k_C n_E N_F - k_S n_R \tag{21}$$

As before, pure char fragments are governed by

$$\frac{dn_P}{dt} = k_S n_R + k_C N_F^2 \tag{22}$$

The second depletion term of eq 20 is the source term for free monomer. The free monomer sinks are conversion to tar and reattachment to a bridge end, a char segment,

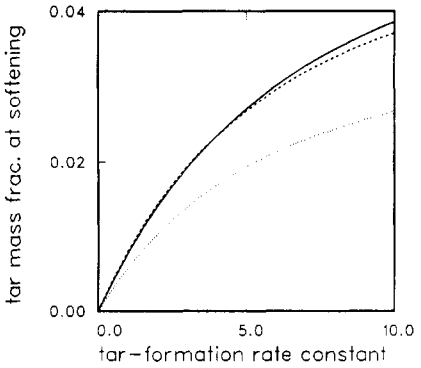

Figure 6. Tar mass fraction N_T at softening vs. tar-formation rate coefficient k_T, computed with the Bethe-lattice model with coordination number z = 3 (solid), 4 (dashed), and 5 (dotted).

a pure char fragment, or another monomer. The rate equation is

$$\frac{dN_F}{dt} = k_S n_E - k_C(n_E + n_R + 2n_P)N_F - 2k_C N_F^2 - k_T N_F \quad (23)$$

where, as before, the tar species is governed by

$$\frac{dN_T}{dt} = k_T N_F \quad (24)$$

The rate equations 20–24, in conjunction with the algebraic relation 19, eq 9 for K, and the initial conditions $N_U = 1$ and $n_E = n_R = n_P = N_C = N_F = N_T = 0$, constitute a well-posed initial-value problem. The char mass fraction is again determined by the mass closure

$$N_U + N_F + N_T + N_C = 1 \quad (25)$$

It is readily verified that the initial-value problem reduces to that of section 3 for $z = 2$.

Numerical solution of the initial-value problem for z values greater than 2 yields qualitative trends analogous to those of section 4. Computed results for parameter assignments motivated by the application to coal devolatilization are presented elsewhere.[8] Here we focus on an aspect of coal-conversion phenomenology which is represented only in networks with $z > 2$. Namely, partially reacted, devolatilizing particles of certain coals (in particular, bituminous coals) exhibit sudden plasticization or softening,[13] an effect whose physicochemical origin is poorly understood. In the context of the macromolecular picture of coal, we interpret softening as a loss of structural integrity (i.e., global connectedness) of the macromolecule, or qualitatively, a time-reversed sol–gel transition. Motivated by the modern theory of gelation,[14] we associate the softening transition with the percolation threshold[15] of the network representing the coal macromolecule.

For the Bethe lattice with coordination number z, loss of global connectedness occurs when the fraction K of broken bridges reaches a critical value[10]

$$K_c = \frac{z-2}{z-1} \quad (26)$$

(For $z = 2$, this expression gives the expected but physically uninteresting result that an infinite linear chain becomes disconnected immediately). On the basis of this criterion, the computed value of N_T at the onset of softening is plotted for several z values in Figure 6 vs. k_T (assumed constant in time) for $k_S = k_C = 1$. The results, which provide a measure of the extent of weight loss at softening, indicate significant sensitivity to the tar formation rate. For given z, the mass fraction N_U of unreacted coal at softening is almost constant (to within 0.1%) over the range of k_T indicated in the figure. For z = 3, 4, and 5, N_U at softening is 0.938, 0.943, and 0.959, respectively, over the indicated range of k_T.

6. Discussion

In its most general formulation, the network model of polymer bond scission with irreversible reattachment of free monomers can represent a variety of phenomena associated with pyrolitic degradation. Here we have focused on transient and ultimate product yields under the influence of an alternate pathway for free monomer depletion, namely tar formation. Specializing to linear chains, a hierarchy of rate equations has been obtained whose solution can also provide information concerning the size distribution of fragments, which may be of interest with respect to species transport and other physical properties. For a more general class of networks, rate equations have been formulated only for species lumps (char, tar, unreacted polymer, etc.). Although analytical results are available for the evolving fragment-size distribution produced by random scission of branched networks,[10] inclusion of reattachment appears to render the problem intractable by methods other than computer simulation.

The percolation threshold of the branched network has been interpreted as the softening transition observed during coal devolatilization. Although percolation criteria for other physicochemical transformations during coal conversion have proven successful in correlating experimental data,[16-19] studies of softening have not yet provided sufficient data to test the proposed mechanism in this instance. Recent advances in experimental technique[20] offer encouragement that suitable data will eventually be obtained.

A qualitative aspect omitted from the present formulation is the phenomenon of resolidification, presumably due to a gelation-like transition associated with the growing char network. Of particular interest is the criterion for resolidification to occur before the softening transition. Such a criterion could formalize the phenomenological distinction between softening and nonsoftening coals. Neither the means nor the phenomenological basis yet exist for modeling the char network other than as a collection of linear segments and fragments, so a predictive capability for resolidification is lacking.

The linear-chain formulation of the model has been used previously to extrapolate product yields based on measurements over a limited range of conditions during coal devolatilization.[6] The predictions obtained by this extrapolation are in good agreement with measurements over a much wider range of conditions.[6-8] In particular, trends governing the dependence of char and tar yields on heating rate are reproduced. The exemplary solutions presented here highlight the specific mechanisms that account for these trends within our modeling framework. Since the phenomenology underlying the model is generic to many pyrolysis processes, these mechanisms may also be pertinent to applications other than the coal devolatilization process emphasized here.

Acknowledgment. This research was supported by the Division of Engineering and Geosciences, Office of Basic Energy Sciences, U. S. Department of Energy.

References and Notes

(1) van Dongen, P. G. J.; Ernst, M. H. *J. Stat. Phys.* **1984**, *37*, 301.
(2) Family, F.; Meakin, P.; Deutch, J. M. *Phys. Rev. Lett.* **1986**, *57*, 727.

(3) Ziff, R. M.; McGrady, E. D. *J. Phys. A.* **1985**, *18*, 3027; *Macromolecules* **1986**, *19*, 2513.
(4) Niksa, S.; Kerstein, A. R. *Combust. Flame* **1986**, *66*, 95.
(5) Given, P. H. In *Coal Science*; Gorbaty, M. L., Larsen, J. W., Wender, I., Eds.; Academic: Orlando, FL, 1984; Vol. 3 p 65.
(6) Niksa, S. *Combust. Flame* **1986**, *66*, 111.
(7) Niksa, S.; Kerstein, A. R.; Fletcher, T. H. *Combust. Flame*, in press.
(8) Niksa, S.; Kerstein, A. R. *Fuel*, in press.
(9) Davidson, R. M. *Molecular Structure of Coal*; IEA Coal Research: London, 1980.
(10) Fisher, M. E.; Essam, J. W. *J. Math. Phys.* **1961**, *2*, 609.
(11) Zallen, R. *The Physics of Amorphous Solids*; Wiley: New York, 1983.
(12) Wilks, S. S. *Mathematical Statistics*; Wiley: New York, 1962.
(13) Habermehl, D.; Orywal, F.; Beyer, H.-D. In *Chemistry of Coal Utilization*; Elliot, M. A., Ed.; Wiley: New York, 1981; 2nd Suppl. Vol. p 317.
(14) Stauffer, D.; Coniglio, A.; Adam, M. *Adv. Polym. Sci.* **1982**, *44*, 103.
(15) Stauffer, D. *Introduction to Percolation Theory*; Taylor and Francis: London, 1985.
(16) Kerstein, A. R.; Niksa, S. *Int. Combust. Symp., 20th* **1984**, 941.
(17) Reyes, S.; Jensen, K. F. *Chem. Eng. Sci.* **1986**, *41*, 333.
(18) Reyes, S.; Jensen, K. F. *Chem. Eng. Sci.* **1986**, *41*, 345.
(19) Kerstein, A. R.; Edwards, B. F. *Chem. Eng. Sci.*, in press.
(20) Fong, W. S.; Khalil, Y. F.; Peters, W. A.; Howard, J. F. *Fuel* **1986**, *65*, 195.

Quantitative Investigation of the Amorphous and Crystalline Components in *trans*-1,4-Polybutadiene from Solution. 1. Effects of Crystallization Temperature and Concentration

Pei-guo Wang and Arthur Woodward*

Department of Chemistry, The City College and The Graduate School, The City University of New York, New York, New York 10031. *Received December 2, 1986*

ABSTRACT: *trans*-1,4-Polybutadiene (TPBD) fractions (M_v = 7000–36 000) with a 1% cis content were crystallized from solution as a function of crystallization solvent, temperature, and concentration. The resulting structures were characterized quantitatively by using epoxidation in suspension followed by carbon-13 NMR measurement in solution, which yields the fraction reacted and the unreacted and reacted block lengths, *A* and *B*, respectively. Agreement between the fraction epoxidized and the noncrystalline fraction from density measurement was obtained. Evidence for the rejection of cis units from the *trans*-polybutadiene crystal core was found from the carbon-13 NMR studies. Although the amorphous (surface) fraction remains constant, *A*, equated to the number of monomer units per crystal traverse, and *B*, equated to the average number of monomer units per fold, increase with crystallization temperature. *A* and *B* remain constant with a change in morphology from single lamellar to multilamellar and with crystallization concentration from 0.05% to 5% w/v. The average number of TPBD units rejected from the crystal core when cis unit rejection occurs is estimated and the average length of a fold containing no cis unit is found to be 3–5 units.

Introduction

The crystallization of flexible-chain polymers from solution yields relatively thin lamellar structures with an appreciable amorphous component residing at the large faces.[1] In these lamellas the chain direction is nearly perpendicular to the large faces and the long-chain nature of linear polymers necessitates chain folding at these faces. Considerable physical and chemical evidence has been gathered to support the chain-folding concept, but a method for the direct determination of the fold size in single lamellas has only recently been forthcoming.[2,3] The direct determination has been carried out on two polydienes, *trans*-1,4-polybutadiene[2] and *trans*-1,4-polyisoprene.[3] The method used involves a chemical reaction, such as epoxidation,[2-5] hydrochlorination,[6] or bromination,[7,8] at low temperatures with the available double bonds at the lamellar surfaces of the sample suspended in a solution of the low molecular weight reactant. The polymeric reaction products are then analyzed in solution by using carbon-13 nuclear magnetic resonance.

For this method to give a correct fold length for single lamellas, as well as the correct crystalline stem length, reaction must occur with all of the double bonds in the folds, the molecular weight must be high or a correction made for noncrystallizing chain ends, and appreciable penetration of the crystal core must not occur. One method of monitoring the reaction is by comparison of the fraction reacted with the amorphous fraction obtained by using an appropriate physical method, such as density[2-6] or solid-state carbon-13 NMR.[9] For a number of the preparations reported to date, discrepancies in the fraction reacted and in the noncrystalline fraction have been reported;[2,6,9] also in some cases excessive damage to lamellas has been observed by electron microscopy.[5,8] Further study of reaction conditions, particularly with respect to the reaction medium and reactant concentration, was necessary in order to correct these problems.

It is of interest to investigate the effects of molecular weight, crystallization conditions and the morphology on the average number of monomer units per fold and crystal stem length since few data are available. To date only three TPBD preparations, studied by using the chemical reaction/carbon-13 NMR method, have been reported on and since only one of these gave agreement between the fraction reacted and the amorphous fraction from density measurements,[2] a more detailed investigation of this polymer was in order. A study was initiated of the structures obtained by solution crystallization of relatively low molecular weight fractions (M_v = 7000 to 3.6 × 10^4) of high trans content 1,4-polybutadiene obtained by $RdCl_3$-initiated emulsion polymerization.[10,11] Crystallization was carried out at various temperatures using two solvents of different polarities and as a function of concentration in one of these solvents. Morphology was studied by using transmission and scanning electron microscopy and the crystalline/amorphous content obtained by density measurement. An epoxidation reaction of the double bonds at the lamellar surfaces was carried out in suspension at 0 °C using *m*-chloroperbenzoic acid and the resulting products were analyzed by 50 MHz carbon-13

0024-9297/87/2220-1818$01.50/0